ChemComm

Phosphinate-Containing Rhodol and Fluorescein Scaffolds for the Development of Bioprobes

Journal:	*ChemComm*
Manuscript ID	CC-COM-03-2019-002492.R1
Article Type:	Communication

Journal Name

COMMUNICATION

Phosphinate-Containing Rhodol and Fluorescein Scaffolds for the Development of Bioprobes

Yuan Fang,[a] Gillian N. Good,[a,b] Xinqi Zhou,[a] and Cliff I. Stains[a,*]

eceived 00th January 20xx,
Accepted 00th January 20xx

DOI: 10.1039/x0xx00000x

www.rsc.org/

A series of phosphinate-containing rhodol and fluorescein dyes are disclosed. These new fluorophores increase the color palette of phosphinate-based xanthenes in the far-red spectral region. The new chemical functionality of these scaffolds is leveraged to produce a sensitive, no-wash imaging probe for cellular esterase activity. The reported phosphinate-containing dyes provide platforms for the further development of imaging probes and self-reporting delivery vehicles.

Small molecule-based fluorescent probes represent attractive alternatives to fluorescent proteins for microscopy studies.[1-3] Nonetheless, there is a need for the further development of red-shifted, photostable probes in order to enable the further development of robust bioprobes for imaging experiments. Towards this goal, recent efforts have focused on the introduction of heteroatoms into the bridging position of xanthene scaffolds.[4-18] Our lab's approach to this problem involves replacement of the bridging oxygen atom in the rhodamine scaffold with a phosphinate functionality (Fig. 1).[19] The resulting Nebraska Red (**NR**) fluorophores retain the brightness and photostability of the rhodamine scaffold, while displaying > 110 nm shifts in excitation and emission. Furthermore, the unique chemistry of the phosphinate functional group allows for the construction of new enzymatic probes,[20] self-reporting small molecule delivery platforms,[19] and provides inspiration for the development of new approaches for obtaining ratiometric probes.[21] Building upon this, we sought the further increase the chemical functionality of **NR** dyes, through the synthesis and evaluation of rhodol- and fluorescein-based **NR** derivatives (Fig. 1). Importantly the phenol group present in these rhodol and fluorescein dyes provides a new chemical handle that can be leveraged to construct sensitive, red-shifted enzyme-activated probes for cellular imaging studies.[22-25]

Towards this goal, we first investigated synthetic routes capable of efficiently yielding rhodol and fluorescein **NR** derivatives. When compared to the synthesis of classical rhodamine dyes, insertion of phosphorous at the bridging position decreases the yield of the resulting fluorophore.[9,19,26] Additional synthetic challenges arise in the case of fluorescein (due to the increased electron withdrawing capacity of the phenol group)[10] and rhodol (due to the need to construct an asymmetric structure).[27,28] During our investigation of different synthetic routes, the Yamaguchi group reported the direct conversion of phosphine oxide-containing rhodamines to rhodol and fluorescein via a hydrolytic deamination reaction under basic conditions (pH > 10).[29] As an initial examination of this route in the context of **NR** dyes, we incubated $\mathbf{NR_{700}}$, a phosphinate ester-based tetramethylrhodamine derivative, with 0.1 M NaOH. After 3 h the products of the reaction were purified by HPLC, yielding the hydrolyse product ($\mathbf{NR_{666}}$) and the corresponding rhodol product ($\mathbf{NR_{630}}$, Fig. S1 and Scheme S1 ESI). Upon incubation of $\mathbf{NR_{700}}$ with a 1 M solution of NaOH, instead of conversion to fluorescein we observed a rapid decrease of the color of the solution. This is likely due to attack at the C-9 position of the fluorophore as observed previously (Scheme S1, ESI).[29] In support of this hypothesis, we observed a restoration of the solutions color upon addition of 2 M HCl. Nonetheless, we were very encouraged by the potential of this route to afford rhodol and fluorescein **NR** derivatives.

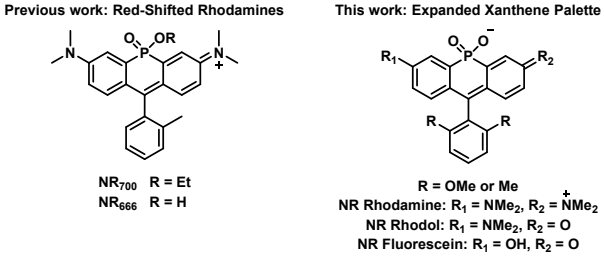

Fig. 1 Structures of xanthene-based Nebraska Red family members.

[a] *Department of Chemistry, University of Nebraska-Lincoln, Lincoln, NE 68588, USA. E-mail: cstains2@unl.edu*
[b] *Department of Chemistry, Millersville University, Millersville, Pennsylvania 17551, United States*

†Electronic Supplementary Information (ESI) available: experimental details, synthesis and characterization of new compounds, and supplementary figures. See DOI: 10.1039/x0xx00000x

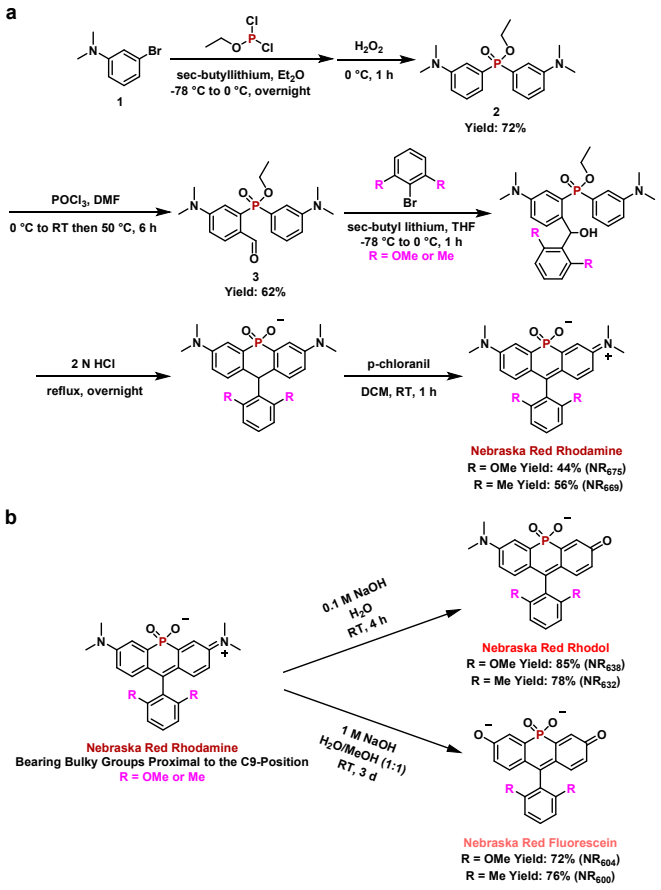

Scheme 1 (a) Synthesis of phosphinate-based **NR** rhodamine analogues. (b) Direct transformation of **NR** rhodamine to **NR** rhodol or **NR** fluorescein.

In order to protect the C-9 position from nucleophilic attack, we adopted previous strategies for introduction of bulky groups into xanthenes,[29,30] incorporating dimethyl or dimethoxy groups at the C-2′ and C-6′ of our **NR** dyes (Fig. 1). Our previously reported route to **NR** rhodamine analogues, relied on the condensation of 3-bromo-N,N-dimethylaniline with benzaldehydes[19,21] or the use of a xanthone precursor[10,12,19,31]. However, as mentioned above, these routes result in relatively low yields of the target fluorophores. Building upon a previously described route for phosphine oxide fluorophores, we found that yields of **NR** rhodamines could be significantly increased by first treating 3-bromo-N,N-dimethylaniline with sec-butyllithium and exposing the resulting lithiated reagent to ethyl dichlorophosphite.[26] Subsequent oxidation with a 50% H_2O_2 solution yielded the phosphinate-bridged intermediate (**2**, Scheme 1a). A subsequent Vilsmeier-Haack reaction was used to generate the key intermediate **3**. Reaction of **3** with the appropriate lithiated 2,6-disubstituted phenyl reagents (dimethyl or dimethoxy) generated the corresponding secondary alcohol, which was directly treated with 2 M HCl under reflux overnight. Finally, p-chloranil was used to generate the **NR** rhodamine analogues containing bulky substituents proximal to the C-9 position. Compared to our previously reported routes,[19] the newly developed intermediate **3** is accessible in relatively higher yields, leading to a ≥ 4-fold increase in the yield of **NR** rhodamines.

With the **NR** rhodamine analogues in-hand, we reassessed the ability to directly generate rhodol and fluorescein derivatives upon treatment with NaOH. Upon exposure to 0.1 M NaOH, the color of the solution quickly changed from green to purple, indicating the generation of **NR** rhodol (Scheme 1b). Monitoring by HPLC indicated that the reaction was complete after 4 hrs. As expected, the generation of **NR** fluorescein required a longer reaction time (3 days) and a higher concentration of base (1 M).[29] After purification by HPLC, the structures of all six **NR** derivatives were confirmed by NMR and mass spectrometry (see ESI).

The photophysical properties of the **NR** rhodamine, rhodol, and fluorescein derivatives were assessed in PBS (10 mM, pH = 7.4) (Fig. 2a-c). The **NR** rhodamine derivatives showed the longest absorption and emission wavelengths, similar to our previously reported analogues.[19] However, the **NR** rhodol and **NR** fluorescein derivatives displayed 35 and 70 nm blue-shifts, respectively relative to **NR** rhodamine. Comparison to the spectral properties of Tokyo Green[32], containing oxygen at the bridging position, indicated that introduction of the phosphinate in **NR** fluorescein resulted in a ≥ 109 nm red-shift.

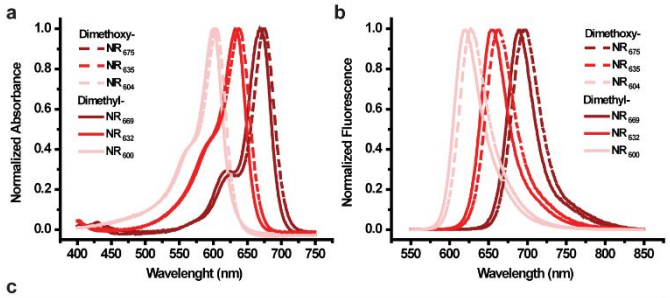

c

Dyes		λ_{ex} (nm)	λ_{em} (nm)	Stokes Shift (nm)	ε (M^{-1}·cm^{-1})	Φ	Brightness (ε·Φ) (M^{-1}·cm^{-1})	pK_a
Rhodamine	NR_{675}	675	695	20	73,200	0.24	17,568	≤ 0.52
	NR_{669}	669	689	20	77,200	0.30	23,160	≤ 0.59
Rhodol	NR_{638}	638	662	24	55,630	0.21	11,682	5.16
	NR_{632}	632	655	23	63,970	0.26	16,632	5.20
Fluorescein	NR_{604}	604	627	23	45,740	0.48	21,955	6.71
	NR_{600}	600	619	19	67,570	0.68	45,948	6.75
	Tokyo Magenta	582	598	16	110,000	0.42	46,200	6.8
	Tokyo Green	491	510	19	85,000	0.85	72,250	6.2

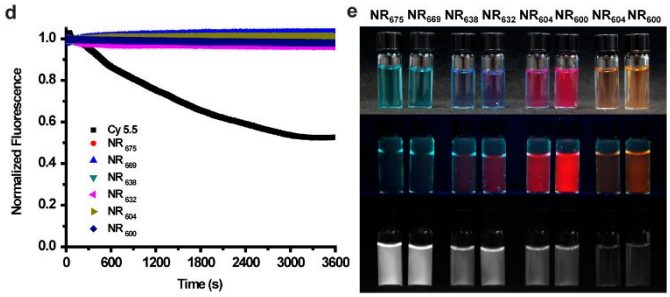

Fig. 2 Photophysical properties and pK_as of **NR** family members. All experiments were conducted in PBS buffer (10 mM, pH = 7.4 containing 1% DMSO). (a) Normalized absorption spectra. (b) Normalized emission spectra. (c) Summary of optical parameters including previously reported values for Tokyo Magenta[5] and Tokyo Green[32]. (d) Photostability in comparison to Cy 5.5. (e) Images corresponding to each dye solution. From top to bottom: white-light image, fluorescent image under a UV lamp (254 nm), and a NIR image with a 680 nm filter. From left to right: NR_{675}, NR_{669}, NR_{638}, NR_{632}, NR_{604}, and NR_{600} in PBS buffer as well as NR_{604} and NR_{600} in buffer at pH = 4.0.

Among the **NR** family members, the dimethoxy analogues were slightly red-shifted compared to their dimethyl counterparts, while the dimethyl **NR** analogues displayed relatively higher brightness (ε × ϕ) with the fluorescein dimethyl derivative (**NR_{600}**) displaying the overall the highest brightness. These **NR** dyes displayed blue-shifted excitation and emission maxima as well as increased brightness compared to previously reported phosphine oxide-based fluorophores (Table S1, ESI).[10,29]

Next, we investigated the equilibrium between protonated and deprotonated forms of the rhodol and fluorescein derivatives. Absorption of the **NR** rhodol and **NR** fluorescein dyes at varying pHs was recorded (Fig. S2, ESI). From this data, the **NR** rhodol derivatives exhibited a pK_a of ~ 5.2 while the pK_as for the **NR** fluorescein derivatives was ~ 6.7. Last, the photostability of **NR** family members was compared to Cy 5.5 using continuous irradiation for 1 h (Fig. 2d). Gratifyingly, all six **NR** dyes showed virtually no evidence of photobleaching, compared to a 50% decrease in Cy 5.5 fluorescence under the same conditions. Thus, these new **NR** derivatives provide a robust, tuneable palette of fluorescent reagents with emissions ranging from the far-red to near-infrared (NIR) region (Fig. 2e).

To highlight to utility of these new **NR** family members, we sought to develop a sensitive bioprobe for imaging enzymatic activity. For this application, we chose the dimethyl phosphinate-based fluorescein **NR_{600}**, due to its relative brightness. Importantly, previous work has clearly demonstrated the utility of acetoxymethyl (AM) ether groups for masking phenol functionalities within fluorophores.[23-25,33] The resulting AM-protected probes display low background fluorescence, high chemical stability, and are readily cleaved by cellular esterases producing a turn-on fluorescent probe for esterase activity. Based on our previous results, we also anticipated that the negatively charged phosphinate of **NR_{600}** would prevent the fluorophore from entering cells.[19] Thus, we envisioned a diAM-protected version of **NR_{600}**, termed **diAM-NR_{600}** (Fig. 3a). To examine the chemical stability of **diAM-NR_{600}**, an *in vitro* assay was conducted by monitoring the fluorescence generated by **diAM-NR_{600}** over a period of 1 hr (Fig. 3b). In the presence of pig liver esterase (PLE) we observed a clear, 13.8-fold increase in fluorescence that stabilized after 10 min. However, in the presence of PBS alone virtually no increase in fluorescence was observed. Moreover, exposure to BSA or cell culture media containing 10% FBS produced relatively low background fluorescent signal (2.2- and 2.9-fold respectively). These data clearly indicate that **diAM-NR_{600}** can act as an esterase substrate, forming **NR_{600}** as a fluorescent product.

To interrogate the ability of **diAM-NR_{600}** to act as a no wash probe for cellular esterase activity, HeLa cells were incubated with the esterase probe and Cell Tracker Green CMFDA, in order to verify localization. Cells were then imaged, without washing, using confocal microscopy (Fig. 4a). Indeed, the formation of **NR_{600}** in the cytosol could clearly be observed within cells (Fig. S3a, ESI), yielding a 10-fold increase in signal over background (Fig. 4b). Similar signal to noise was obtained in HeLa cells that were washed prior to imaging (Fig. S3b, ESI). In addition, formation of **NR_{600}** was also observed in the cytosol of NIH-3T3 and RAW 264.7 cells, indicating the generality of **diAM-NR_{600}** (Fig. S4 and S5, ESI). Decreased

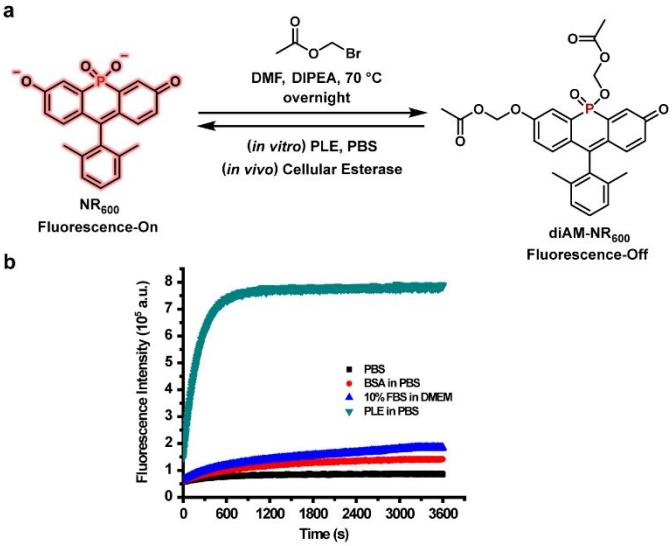

Fig. 3 (a) Synthesis of the esterase sensor **diAM-NR_{600}**. (b) *In vitro* stability of **diAM-NR_{600}** (5 μM) in PBS (10 mM, pH = 7.4) alone or in the presence of BSA (0.2 units) or PLE (0.2 unit). The fluorescence of **diAM-NR_{600}** in cell culture media (DMEM with 10% FBS) is also shown. Fluorescence emission at 619 nm was monitored using excitation at 600 nm.

nuclear localization of **NR_{600}** was consistently observed relative to Cell Tracker Green CMFDA (a fluorescein derivative), indicating a potential difference in the nuclear accumulation of these dyes. Toxicity assays also clearly demonstrated that **diAM-NR_{600}** was not toxic at concentrations up to 10 μM (Fig. S6). These experiments verify the ability of **diAM-NR_{600}** to act as a far-red emitting, no-wash probe for cellular esterase activity.

In summary, we have broadened the color palette of our **NR** dyes to include rhodol and fluorescein derivatives. The resulting **NR** rhodol and fluorescein dyes display significantly red-shifted fluorescence relative to their oxygen analogues and display increased photostability compared to commonly used labels

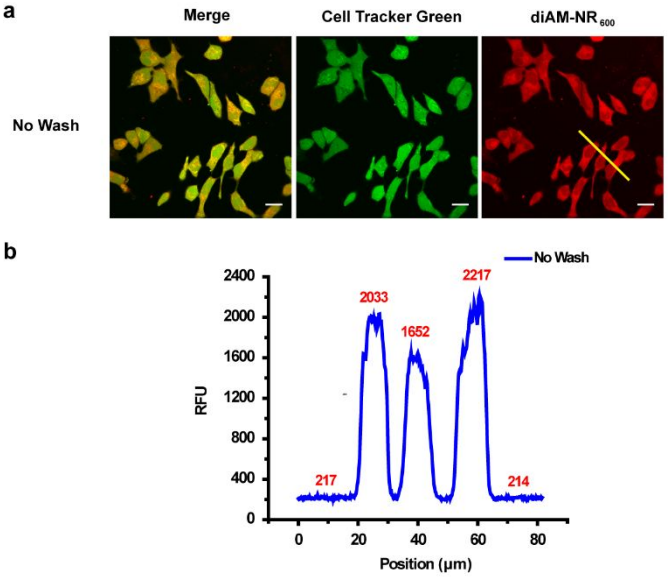

Fig. 4 (a) Confocal fluorescence microscopy imaging of HeLa cells incubated with 0.6 μM Cell Tracker Green CMFDA for 20 min followed by 0.6 μM **diAM-NR_{600}** for 30 min (Scale bar: 20 μm). (b) Quantification of fluorescence intensity from panel a (yellow line in red channel).

such as Cy5.5. The new chemical functionality afforded by these scaffolds enabled the development of a red-shifted, no-wash probe for cellular esterase activity. Current efforts in our lab are focused on lowering the pK_a of the **NR** fluorescein series to further increase the brightness at physiological pH. These new **NR** dye scaffolds also provide the starting point for the development of additional probes for enzymatic activity,[34] reagents for advanced imaging experiments,[35-37] and self-reporting delivery reagents.[19]

We gratefully acknowledge the Morrison Microscopy Core Research Facility and Prof. Christian Elowsky for assistance with confocal fluorescence microscopy as well as Prof. Edward Harris for use of cell culture equipment. We also thank the Research Instrumentation/NMR facility and the Nebraska Center for Mass Spectrometry for assistance with characterization of new compounds. This work was funded by the NIH (R35GM119751), NSF (CHE-1757957), and the University of Nebraska-Lincoln. The content of this work is solely the responsibility of the authors and does not necessarily represent the official views of the NIH.

Conflicts of interest

The authors declare no conflicts of interest.

Notes and references

1 L. D. Lavis and R. T. Raines, *ACS Chem. Biol.*, 2008, **3**, 142-155.
2 L. D. Lavis and R. T. Raines, *ACS Chem. Biol.*, 2014, **9**, 855-866.
3 L. D. Lavis, *Biochemistry*, 2017, **56**, 5165-5170.
4 Y. Koide, Y. Urano, K. Hanaoka, T. Terai and T. Nagano, *ACS Chem. Biol.*, 2011, **6**, 600-608.
5 T. Egawa, Y. Koide, K. Hanaoka, T. Komatsu, T. Terai and T. Nagano, *Chem. Commun.*, 2011, **47**, 4162-4164.
6 Y. Koide, Y. Urano, K. Hanaoka, W. Piao, M. Kusakabe, N. Saito, T. Terai, T. Okabe and T. Nagano, *J. Am. Chem. Soc.*, 2012, **134**, 5029-5031.
7 Y. Koide, M. Kawaguchi, Y. Urano, K. Hanaoka, T. Komatsu, M. Abo, T. Terai and T. Nagano, *Chem. Commun.*, 2012, **48**, 3091-3093.
8 J. B. Grimm, A. J. Sung, W. R. Legant, P. Hulamm, S. M. Matlosz, E. Betzig and L. D. Lavis, *ACS Chem. Biol.*, 2013, **8**, 1303-1310.
9 X. Chai, X. Cui, B. Wang, F. Yang, Y. Cai, Q. Wu and T. Wang, *Chem. Eur. J.*, 2015, **21**, 16754-16758.
10 A. Fukazawa, S. Suda, M. Taki, E. Yamaguchi, M. Grzybowski, Y. Sato, T. Higashiyama and S. Yamaguchi, *Chem. Commun.*, 2016, **52**, 1120-1123.
11 J. B. Grimm, T. D. Gruber, G. Ortiz, T. A. Brown and L. D. Lavis, *Bioconjug. Chem.*, 2016, **27**, 474-480.
12 J. Liu, Y. Q. Sun, H. Zhang, H. Shi, Y. Shi and W. Guo, *ACS Appl. Mater. Inter.*, 2016, **8**, 22953-22962.
13 J. B. Grimm, T. A. Brown, A. N. Tkachuk and L. D. Lavis, *ACS Cent. Sci.*, 2017, **3**, 975-985.
14 W. Piao, K. Hanaoka, T. Fujisawa, S. Takeuchi, T. Komatsu, T. Ueno, T. Terai, T. Tahara, T. Nagano and Y. Urano, *J. Am. Chem. Soc.*, 2017, **139**, 13713-13719.
15 L. V. Lutkus, H. E. Irving, K. S. Davies, J. E. Hill, J. E. Lohman, M. W. Eskew, M. R. Detty and T. M. McCormick, *Organometallics*, 2017, **36**, 2588-2596.
16 T. Hirayama, A. Mukaimine, K. Nishigaki, H. Tsuboi, S. Hirosawa, K. Okuda, M. Ebihara and H. Nagasawa, *Dalton T.*, 2017, **46**, 15991-15995.
17 C. Fischer and C. Sparr, *Angew. Chem. Int. Ed.*, 2018, **57**, 2436-2440.
18 F. Deng and D. Xu, *Chinese Chem. Lett.*, **In Press**, DOI: 10.1016/j.cclet.2018.1012.1012.
19 X. Zhou, R. Lai, J. R. Beck, H. Li and C. I. Stains, *Chem. Commun.*, 2016, **52**, 12290-12293.
20 X. Chai, J. Xiao, M. Li, C. Wang, H. An, C. Li, Y. Li, D. Zhang, X. Cui and T. Wang, *Chem. Eur. J.*, 2018, **24**, 14506-14512.
21 X. Zhou, L. Lesiak, R. Lai, J. R. Beck, J. Zhao, C. G. Elowsky, H. Li and C. I. Stains, *Angew. Chem. Int. Ed.*, 2017, **56**, 4197-4200.
22 L. D. Lavis, T. Y. Chao and R. T. Raines, *ACS Chem. Biol.*, 2006, **1**, 252-260.
23 L. D. Lavis, T. Y. Chao and R. T. Raines, *Chem Sci*, 2011, **2**, 521-530.
24 L. Tian, Y. Yang, L. M. Wysocki, A. C. Arnold, A. Hu, B. Ravichandran, S. M. Sternson, L. L. Looger and L. D. Lavis, *Proc. Natl. Acad. Sci. U.S.A.*, 2012, **109**, 4756-4761.
25 W. Chyan and R. T. Raines, *ACS Chem. Biol.*, 2018, **13**, 1810-1823.
26 A. Fukazawa, J. Usuba, R. A. Adler and S. Yamaguchi, *Chem. Commun.*, 2017, **53**, 8565-8568.
27 M. V. Sednev, C. A. Wurm, V. N. Belov and S. W. Hell, *Bioconjug. Chem.*, 2013, **24**, 690-700.
28 A. Roth, H. Li, C. Anorma and J. Chan, *J. Am. Chem. Soc.*, 2015, **137**, 10890-10893.
29 M. Grzybowski, M. Taki and S. Yamaguchi, *Chem. Eur. J.*, 2017, **23**, 13028-13032.
30 Z. Lei, X. Li, Y. Li, X. Luo, M. Zhou and Y. Yang, *J. Org. Chem.*, 2015, **80**, 11538-11543.
31 Q. A. Best, N. Sattenapally, D. J. Dyer, C. N. Scott and M. E. McCarroll, *J. Am. Chem. Soc.*, 2013, **135**, 13365-13370.
32 Y. Urano, M. Kamiya, K. Kanda, T. Ueno, K. Hirose and T. Nagano, *J. Am. Chem. Soc.*, 2005, **127**, 4888-4894.
33 S. R. Levine and K. E. Beatty, *Chem. Commun.*, 2016, **52**, 1835-1838.
34 G. R. Casey and C. I. Stains, *Chem. Eur. J.*, 2018, **24**, 7810-7824.
35 M. Martineau, A. Somasundaram, J. B. Grimm, T. D. Gruber, D. Choquet, J. W. Taraska, L. D. Lavis and D. Perrais, *Nat. Commun.*, 2017, **8**.
36 C. Wang, M. Taki, Y. Sato, A. Fukazawa, T. Higashiyama and S. Yamaguchi, *J. Am. Chem. Soc.*, 2017, **139**, 10374-10381.
37 M. Grzybowski, M. Taki, K. Senda, Y. Sato, T. Ariyoshi, Y. Okada, R. Kawakami, T. Imamura and S. Yamaguchi, *Angew. Chem. Int. Ed.*, 2018, **57**, 10137-10141.

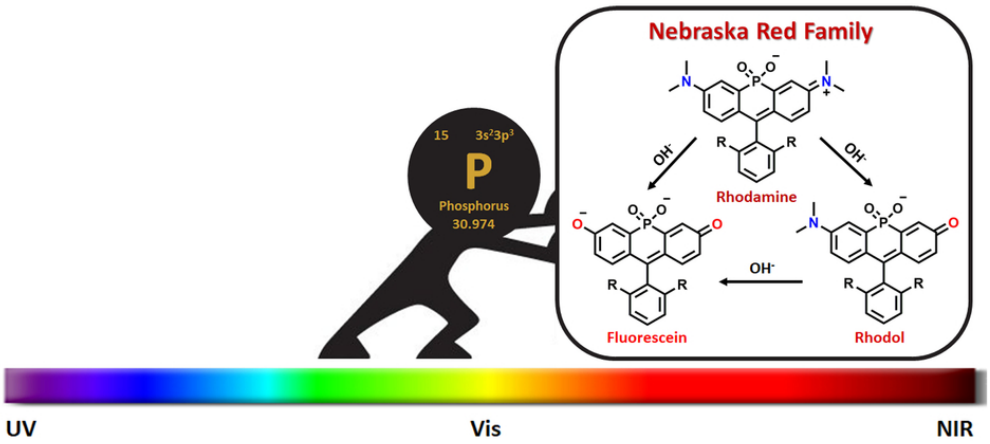

79x38mm (300 x 300 DPI)